Published in final edited form as:
Bioconjug Chem. 2009 March ; 20(3): 432–436. doi:10.1021/bc800422b.

A Novel Method for Direct site-specific Radiolabeling of Peptides Using [^{18}F]FDG

Mohammad Namavari[†], **Zhen Cheng**[†], **Rong Zhang**[‡], **Abhijit De**[†], **Jelena Levi**[†], **Joshua K. Hoerner**[‡], **Shahriar S. Yaghoubi**[†], **Faisal A. Syud**[‡], and **Sanjiv S. Gambhir**[*,†]

[†]Molecular Imaging Program at Stanford (MIPS), Departments of Radiology and Bioengineering, Bio-X Program, Stanford University

[‡]Global Research, General Electric.

Abstract

We have used the well-accepted and easily available 2-[^{18}F]Fluoro-2-deoxyglucose ([^{18}F]FDG) positron emission tomography (PET) tracer as a prosthetic group for synthesis of ^{18}F-labeled peptides. We herein report the synthesis of [^{18}F]FDG-RGD (^{18}F labeled linear RGD) and [^{18}F]FDG-cyclo(RGD^{D}YK) (^{18}F labeled cyclic RGD) as examples of the use of [^{18}F]FDG. We have successfully prepared [^{18}F]FDG-RGD and [^{18}F]FDG-cyclo(RGD^{D}YK) in 27.5% and 41% radiochemical yields (decay corrected) respectively. The receptor binding affinity study of FDG-cyclo(RGD^{D}YK) for integrin $\alpha_v\beta_3$, using $\alpha_v\beta_3$ positive U87MG cells confirmed a competitive displacement with ^{125}I-echistatin as a radioligand. The IC_{50} value for FDG-cyclo(RGD^{D}YK) was determined to be 0.67 ± 0.19μM. High contrast small animal PET images with relatively moderate tumor uptake were observed for [^{18}F]FDG-RGD and [^{18}F]FDG-cyclo(RGD^{D}YK) as PET probes in xenografts models expressing $\alpha_v\beta_3$ integrin. In conclusion, we have successfully used [^{18}F]FDG as a prosthetic group to prepare ^{18}F]FDG-RGD and [^{18}F]FDG-cyclic[RGD^{D}YK] based on a simple one step radiosynthesis. The one step radiosynthesis methodology consists of chemoselective oxime formation between an aminooxy functionalized peptide and [^{18}F]FDG. The results have implications for radiolabeling of other macromolecules and would lead to a very simple strategy for routine pre-clinical and clinical use.

Currently, time-sensitive methods used for ^{18}F-labeling of peptides for positron emission tomography (PET) imaging involve the development of unique ^{18}F-containing prosthetic groups for attachment to the peptides that will likely require significant effort to pervasively implement for routine pre-clinical and clinical application. Therefore, the ability to utilize reagents currently well-accepted and easily available in the PET community at the final formulation step will likely be highly beneficial. The use of 2-[^{18}F]Fluoro-2-deoxyglucose ([^{18}F]FDG) is well-established in clinical PET centers (1) and we show here the potential use of this tracer, without further chemical modifications, to label peptides that can be used to report on one or more biomarkers *in vivo*.

We herein report the synthesis of a ^{18}F-labeled linear trimeric-peptide, [^{18}F]FDG-RGD, and ^{18}F-labeled cyclic trimeric-peptide, [^{18}F]FDG-cyclo(RGD^{D}YK) by using [^{18}F]FDG without further modification. We chose $\alpha_v\beta_3$ integrin and its peptide ligand because the trimeric-peptides sequences argenine-glycine-aspartic acid (RGD) recongnizes the $\alpha_v\beta_3$ integrin found on new blood vessels and tumor cells. RGD peptide binds to $\alpha_v\beta_3$ integrin and

*Author to whom correspondence should be addressed:, Sanjiv Sam Gambhir M.D., Ph.D., Molecular Imaging Program at Stanford, Departments of Radiology and Bioengineering, Bio-X Program, 318 Campus Dr., Clark Center, E-150, Stanford University, Stanford, CA 94305, 650-725-2309 (V), 650-724-4948(Fax), E-mail: sgambhir@stanford.edu.

inhibits angiogenesis (2). The $\alpha_v\beta_3$ integrin is highly expressed in activated endothelial and solid tumor cells (3–4). The synthesis of the radiolabeled peptides utilizes the reaction between the aldehyde functionality in the linear, open form of [^{18}F]FDG with an aminooxy functionality in the peptide to form an oxime bond. The resulting ^{18}F-labeled RGD molecules were evaluated *in vitro* for their binding affinity and ultimately as PET probes in xenograft models expressing $\alpha_v\beta_3$ integrin to demonstrate the integrity of the binders post labeling.

Chemoselective oxime formation between an aminooxy group and a carbonyl functionality has recently been successfully utilized for [^{18}F]-labeling of peptides (5–6), and we hypothesized that it can be used to directly attach [^{18}F]FDG to biomarker-targeted peptides. The highly specific oxime formation between an aminooxy-functionalized peptide and an 4-[^{18}F]fluorobenzaldehdey ([^{18}F]FBA) has previously offered high-yield, two steps synthesis for ^{18}F- labeled peptides (6–9). [^{18}F]FBA can be obtained in a non-optimized radiochemical yield of 50 % in 30 min, with reported radiochemical yields of 60%–80% for the final ^{18}F-peptides. The hypothesis is further supported by a recent report by Wuest *et al*., which reported the oxime formation between [^{18}F]FDG and N-[6-(aminooxy)hexyl]maleimide to create a thiol reactive prosthetic group [^{18}F]FDG-maleimidehexyloxime ([^{18}F]FDG-MHO) in moderately high yield (45–69%) at 100 °C over 15 minutes (10). The basis of this chemistry lies in the fact that at 100 °C, FDG exists in a dynamic equilibrium between its cyclic form and a liner form, where the latter contains an aldehyde functionality at position 1 that can potentially react with the aminooxy functionality under appropriate conditions. We wanted to understand the feasibility of whether such conditions could be translated directly to a targeting peptide while maintaining the peptide's biological efficacy in cell culture and small living subjects.

[^{18}F]FDG-Peptide Conjugation

The synthesis of FDG-RGD and [^{18}F]FDG-RGD were carried out as outlined in scheme 1. The linear aminooxy-RGD (RGD-ONH_2, 2 mg) was incubated with 3.7 equivalents cold FDG in 16 % ethanol in saline (120 μl) in the presence of 0.4 % TFA at 100 °C for 40 min to afford FDG-RGD (E- and Z-oximes) in 39.5 % yield. The formation of E- and Z-oximes was expected. It has been reported that in a similar case, the reaction of glucose with O-(4-nitrobenzyl)-hydroxylamine afforded E and Z-oximes isomers (11). The mass spectrometry (ESI-MS) analysis of the isolated product showed two identical mass peaks of 584.2 ($[M+H]^+$) which correspond to FDG-RGD (E- and Z-oximes) (cal. [M+H] for RGD-FDG is 584.5.). Similarly, aminooxy-RGD (2 mg) was reacted with 4–6 mCi of [^{18}F]FDG in the same condition as above but in 30 minutes to afford [^{18}F]FDG-RGD (E- and Z- oximes) in 27.5 % radiochemical yields based on [^{18}F]FDG (decay corrected). [^{18}F]RGD-FDG oximes were purified by HPLC and used for biological studies. Similar stereochemistry has been observed in the synthesis of ^{18}F-lableled peptide Gluc-s-Dpr ([^{18}F]BOAT)TOACF by using an ^{18}F-benzaldehyde (6).

Likewise, conjugation of FDG and [^{18}F]FDG to cyclo(RGD^{D}YK)-ONH_2 were achieved according to scheme 1. Cyclo(RGD^{D}YK)-ONH_2 (2 mg) was incubated with 5.7 equivalents of FDG in 16 % ethanol in saline (120 μl) and 0.4 % TFA at 100 °C for 60 min to give FDG-cyclo(RGD^{D}YK) (E- and Z-oximes) in 41.4 % yield. The purified FDG-cyclo(RGD^{D}YK) showed two identical mass peaks of 857.35 ($[M+H]^+$) in ESI-MS which are corresponding to FDG-cyclo(RGD^{D}YK) (E- and Z-oximes) (cal. M+H for FDG-cyclo(RGD^{D}YK) is 857.47.). Conjugation of ^{18}FDG to cyclo(RGD^{D}YK)-ONH^2 (2 mg) afforded [^{18}F]FDG-cyclo (RGD^{D}YK) (E- and Z-oximes) in 41% radiochemical yield based on [^{18}F]FDG (decay corrected). [^{18}F]FDG-cyclo(RGD^{D}YK) (E- and Z-) oximes were purified but not separated by HPLC and the two ^{18}F-labeled products (E- or Z-oximes) were isolated as a mixture and analyzed by analytical HPLC (Figure 1). The exact stereochemistry (E- and Z-) of these two products has not been determined yet. We found that under our experimental conditions maximum radiochemical yields were obtained at pH values of 1.5–2.5. When the reaction was

performed at pH 4 in ammonium acetate buffer no significant products were produced. In our previous report (9) we addressed the selectivity of aldehyde towards the aminooxy groups over the amine groups in conjugation of RGD peptides with a simple aldehyde such as 4-flurobenzaldehyde. We found that when for example, two RGD aminooxy-functionalized peptides NH_2OCH_2CO-Arg-Gly-Asp-NH_2 and NH_2OCH_2CO-Lys-Arg-Gly-Asp-NH_2 were reacted at the same condition (8.5–150 equivalents, 45–60 min, 70 °C, pH 4) with 4-flourobenzaldehyde, in each case only one oxime product was formed. It strongly suggests that in conjugation of RGD-ONH_2 or cyclo(RGD^{D}YK)-ONH_2 with FDG oximes are the major products. Similar selectivity was observed by Poethko et al. (6) where they tested the selectivity of 4-[^{18}F]flurobenzaldehyde for aminooxy groups vs. amine groups in amino acids argentine serine, histidine, and lysine both in the presence and the absence of 2-aminooxyacetic acid. The major limitations of our ^{18}F-labeling methodology are the high temperature (100 °C) and acidic pH conditions. High temperature and acidic pH are tolerated for the small unprotected peptides but might not be suitable for the large peptides.

Cell Culture Binding Studies

To determine whether FDG-cyclo(RGD^{D}YK) has similar receptor binding affinity for integrin $\alpha_v\beta_3$ as cyclo(RGD^{D}YK), we studied the receptor binding affinity of FDG-cyclo(RGD^{D}YK) for integrin $\alpha_v\beta_3$, using $\alpha_v\beta_3$ positive U87MG cells. The receptor binding affinity study of FDG-cyclo(RGD^{D}YK) for integrin $\alpha_v\beta_3$, using $\alpha_v\beta_3$ positive U87MG cells confirmed a competitive displacement with ^{125}I-echistatin as a radioligand (Figure 2). The IC_{50} value for FDG-cyclo(RGD^{D}YK) was determined to be 0.67 ± 0.19 μM. The corresponding IC_{50} value of cyclo(RGD^{D}YK) is 0.23 μM (12).This result suggests that fluorine-labeling and the conditions (100 °C and acidic pH) did not have a dramatic affect on its binding affinity.

Biodistribution and Imaging

In order to determine the *in vivo* imaging performance of [^{18}F]-labeled FDG-RGD over alternatively ^{18}F-labeled RGD analogs, we evaluated [^{18}F]FDG-RGD in U87MG tumor bearing nude mice which express $\alpha_v\beta_3$ integrin on both tumor vasculature and tumor cells. In vivo biodistribution of [^{18}F]FDG–RGD in U87MG tumor bearing nude mice (n=6) expressing $\alpha_v\beta_3$ integrin is shown in Table 1. The ratios of tumor to blood, tumor to liver and tumor to kidney at 2 h post injection of the probe are comparable to [^{18}F]Galacto-RGD analog that has been used for biodistribution of [^{18}F]Galacto-RGD in osteosarcoma tumor bearing nude mice which express $\alpha_v\beta_3$ integrin (13). MicroPET images of U87MG tumor bearing nude mice (n=6), 0.5, 1 and 2 hr after tail vein injection of ^{18}F labeled [^{18}F]FDG–RGD probe were obtained. Figure 3 shows the microPET image of one representative mouse. The subcutaneous U87MG mice tumors could be clearly visualized from surrounding background tissue.

To evaluate *in vivo* imaging performance of [^{18}F]FDG-cyclo(RGD^{D}YK) in small living subjects, we investigated biodistribution and microPET imaging of U87MG tumor bearing nude mice expressing $\alpha_v\beta_3$ integrin by using [^{18}F]FDG-cyclo(RGD^{D}YK) as a probe. Biodistribution of [^{18}F]FDG-cyclo(RGD^{D}YK) in U87MG tumor bearing nude mice (n=9) expressing $\alpha_v\beta_3$ integrin is shown in Table 2. The ratios of tumor to blood, tumor to muscle and tumor to liver at 2 h post injection of the probe were 3, 13, and 6 respectively. MicroPET images of U87MG tumor bearing nude mice (n=3), 60 min after tail vein injection of [^{18}F] FDG]-cyclo(RGD^{D}YK) were also obtained. Figure 4 shows the microPET image of one representative mouse. The subcutaneous U87MG mouse tumor could be clearly visualized from surrounding background tissue. Tracer activity within the tumor was determined to be 1.06 ± 0.20 % ID/g, by region of interest (ROI) analysis of the three mice which matches with the value of 0.95 ± 0.4 % ID/g determined by the biodistribution studies (Table 2) and muscle uptake was 0.20 ± 0.12 % ID/g. Although the reasons for the relatively fast clearance and

moderate tumor uptake, after 60 minutes of injection of [^{18}F]FDG-cyclo(RGD^{D}YK) are not clear, the use of ^{18}F labeled dimeric or tetrameric ^{18}FDG labeled RGD should be explored. Recent reports (14–16) on the radiolabeled DOTA conjugated-cyclic-RGD, monomer, dimer and tetramer with ^{64}Cu showed that tetrameric cyclic-RGD peptide tracer had about twice as much tumor uptake than the corresponding dimer. Also, the dimer had significantly higher uptake than the monomer counterpart. Likewise, It has been shown that ^{18}F-labeled dimeric RGD peptide, [^{18}F]FB-E[c(RGDYK)]$_2$ has superior imaging characteristic than the corresponding monomer (17).

Conclusion

We have successfully prepared [^{18}F]FDG-RGD and [^{18}F]FDG-cyclo(RGD^{D}YK) based on a simple one step radiosynthesis by using [^{18}F]FDG as a prosthetic group. The one step radiosynthesis methodology consists of chemoselective oxime formation between an easily synthesized aminooxy functionalized peptide and [^{18}F]FDG. The [^{18}F]FDG labeled RGD peptides can be used to image tumors expressing in living subjects. Imaging of integrin $\alpha_v\beta_3$ expression in living subjects would offer a potentially useful approach to diagnose tumors and their metastasis, to help us better understand tumor angiogenesis and to monitor target specific anti-angiogenesis treatment efficacy. The preliminary mice data support further investigation of the tracers and more comparisons to alternately labeled RGD peptides. The major limitations for generalization of our ^{18}F-labeling methodology are the relatively high temperature (100° C) and acidic pH conditions required. High temperature and acidic pH are tolerated for the small unprotected peptides but might not be suitable for larger peptides. This approach may also be useful for labeling other biomolecules and would lead to a very simple strategy for routine pre-clinical and clinical use. The methodology additionally provides benefits such as the use of unprotected aminooxy precursor and the ability to form oximes in aqueous media, providing easy formulation for *in vivo* use. Indeed, the chemistry has been proven through many biological applications in the synthesis of glycopeptides (18–19), oligonucleotide-peptide conjugates (20–21), complex proteins (from peptide fragments) (22), and conjugation of oligo-ribonucleotides and proteins with metal chelates (23).

Supplementary Material

Refer to Web version on PubMed Central for supplementary material.

ACKNOWLEDGMENT

This work was supported, in part, by Medical Diagnostics, GE Healthcare, National Cancer Institute (NCI) Small Animal Imaging Resource Program (SAIRP) grant R24 CA93862, and NCI In Vivo Cellular Molecular Imaging Center (ICMIC) grant P50 CA114747 (SSG). We also thank Dr. David Dick for [^{18}F] production, Dr. Frederick T. Chin for modification of a GE TRACERlab FX-FN synthetic module for radiosynthesis, Dr. Alan Cuthbertson and Dr. Alex Gibson of GE Healthcare for their review of the manuscript.

LITRATURE CITED

1. Gambhir SS. Molecular imaging of cancer with positron emission tomography. Nat. Rev. Cancer 2002;2:683–693. [PubMed: 12209157]
2. Brooks PC, Clark R. Requirement of vascular integrine $\alpha_v\beta_3$ for angiogenesis. Science 1994;264:569–571. [PubMed: 7512751]
3. Cairns RA, Khokha R, Hill RP. Molecular mechanisms of tumor invasion and metastasis: an integrated view. Curr. Mol. Med 2003;3:659–671. [PubMed: 14601640]
4. Felding-Habermann B. Integrin adhesion receptors in tumor metastasis. Clin. Exp. Metastasis 2003;20:203–213. [PubMed: 12741679]

5. Toyokuni T, Walsh JC, Dominguez A, Phelps ME, Barrio JR, Gambhir SS, Satyamurthy N. Synthesis of a New Hetrobifunctional Linker, N-[4-(Aminooxy)butyl]maleimide, for Facile Access to a Thiol-Reactive ^{18}FLabeling Agent. Bioconjugate Chem 2003;14:1253–1259.
6. Poethko T, Schottelius M, Thumshirn G, Hersel U, Herz M, Henriksen G, Kessler H, Schwaiger M, Wester H-J. Two-step methodology for high yield routine radiohalogenation of peptides, ^{18}F-labeled RGD and octreotide analogs. J. Nucl. Med 2004;45:892–902. [PubMed: 15136641]
7. Berndt M, Pietzsch J, Wuest F. Labeling of low –density lipoproteins: ^{18}F-labeled thio-reactive reagent N-[6-[^{18}F]fluorobenzylidine)aminooxyhexyl]maeimide. Nucl. Med. and Biol 2007;34:5–25. [PubMed: 17210457]
8. Cheng Z, De Jesus OP, Namavari M, De A, Levi J, Webster JM, Zhang R, Lee B, Syud FA, Gambhir SS. Small-Animal PET Imaging of Human Epidermal Growth Factor Receptor Type 2 Expression with Site-Specific ^{18}F-Labeled Protein Scaffold. J Nucl Med 2008;49:804–813. [PubMed: 18413392]
9. Namavari M, De Jesus OP, Cheng Z, De A, Kovacs E, Levi J, Zhang R, Joshua K, Hoerner JK, Grade H, Syud FA, Gambhir SS. Direct Site-Specific Radiolabeling of an Affibody Protein with 4-[^{18}F] Fluorobenzaldehyde via Oxime Chemistry. Molecular Imaging & Biology 2008;10:177–181. [PubMed: 18481153]
10. Berndt M, Pietzsch J, Bergmann R, Wuest F. A Novel role for [^{18}F]FDG: Synthesis and application of a [^{18}F]FDG-based prosthetic group for Peptides and protein labeling. J Nucl Med 2006;47:29.
11. Ramsy SL, Freeman C, Grace PB, Remond JW, MacLeod JK. Mild tagging procedures for the structural analysis of glycans. Carbohydrate. Res 2001;333:59–71.
12. Cai, w; Chen, K.; Li, Z-B.; Gambhir, SS.; Chen, X. Dual-Function Probe for PET and Near-Infrared Fluorescence Imaging of Tumor Vasculature. J Nucl. Med 2007;48:1862–1870. [PubMed: 17942800]
13. Haubner R, Wester HJ, Weber WA, Mang C, Ziegler SI, Goodman SL, Senekowitsch-Schmidtke R, Kessler H, Schwaiger M. Noninvasive imaging of alpha(v)beta3 integrin expression using ^{18}F-labeled RGD-containing glycopeptides and positron emission tomography. Cancer Res 2001;61:1781–1785. [PubMed: 11280722]
14. Chen X, Park R, Tohme M, Shahinian AH, Bading JR, Conti PS. MicroPET and autoradiographic imaging of breast cancer α_v-integrin expression using ^{18}F- and ^{64}Cu-labeled RGD peptide. Bioconjug. Chem 2004;15:41–49. [PubMed: 14733582]
15. Chen X, Liu S, Hou Y, Tohme M, Park R, Bading JR, Conti PS. MicroPET imaging of breast cancer α_v-integrin expression with ^{64}Culabeled dimeric RGD peptides. Mol. Imaging Biol 2004;6:350–359. [PubMed: 15380745]
16. Wu Y, Zhang X, Xiong Z, Cheng Z, Fisher DR, Liu S, Gambhir SS, Chen X. MicroPET Imaging of Glioma α_v-Integrin Expression Using ^{64}Cu Labeled Tetrameric RGD Peptide. J. Nucl. Med 2005;46:1707–1718. [PubMed: 16204722]
17. Chen X, Tohme M, Park R, Hou Y, Bading JR, Conti PS. MicroPET imaging of $\alpha_v\beta_3$-Integrine Expression with ^{18}F-Flabeled dimeric RGD peptide. Mol. Imaging 2004;3:96–104. [PubMed: 15296674]
18. Renaudet O, Dumy P. Chemoselectively Template-Assembled Glycoconjugates as Mimics for Multivalent Presentation of Carbohydrates. Org. Lett 2003;5:243–246. [PubMed: 12556162]
19. Dey S, Sheppard TL. Ketone-DNA: A versatile Postsynthetic DNA decoration Platform. Org. Lett 2001;3:3983–3986. [PubMed: 11735565]
20. Hamma T, Miller PS. 4-(2-Aminooxy)-2-(ethylureido)quinoline-Oligonucleotide Conjugates: Synthesis , Binding Interactions and Derivatization with Peptides. Bioconjug. Chem 2003;14:320–330. [PubMed: 12643742]
21. Zatsepin TS, Stetsenko DA, Arzumanov AA, Romonova EA, Gait MJ, Oretskaya TS. Synthesis of Peptide- Oligonucleotide Conjugates with Single and Multiple Peptide Attached to 2′- Aldehydes through Thiazolidine, Oxime, and Hydrazine Linkages. Biocnjug Chm 2002;13:822–830.
22. Bure C, Leliever D, Delmas A. Identification of by-products from an orthogonal peptide ligation by oxime bonds using spectrometry and tandem mass spectrometry. Rapid Commun Mass Spectrom 2000;14:2158–2164. [PubMed: 11114025]

23. Peuralahti J, Puukka K, Hakala H, Mukkala V-M, Mulari Q, Hurskainen P, Hovinen J. Synthesis of Nonluminescent Lanthanide (III) Chelates Tethered to an Aminooxy Group and their Applicability to Biomolecules Derivatization. Bioconjug. Chem 2002;13:876–880. [PubMed: 12121144]

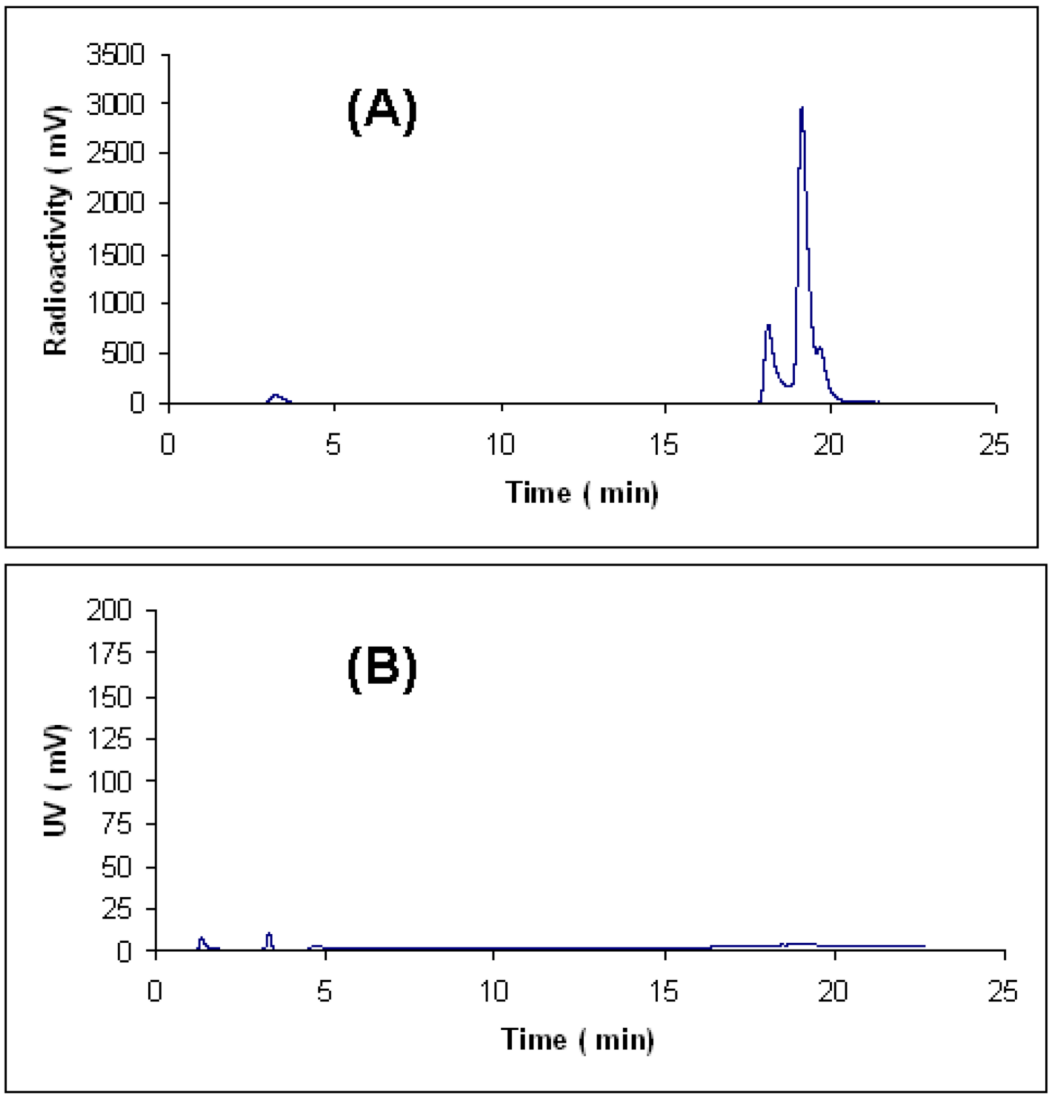

Figure 1.
Analytical HPLC profiles of [^{18}F]FDG-cyclo(RGD^{D}YK) (E-and Z-oximes) after semiprep HPLC. A is radioactive trace and B is UV trace.

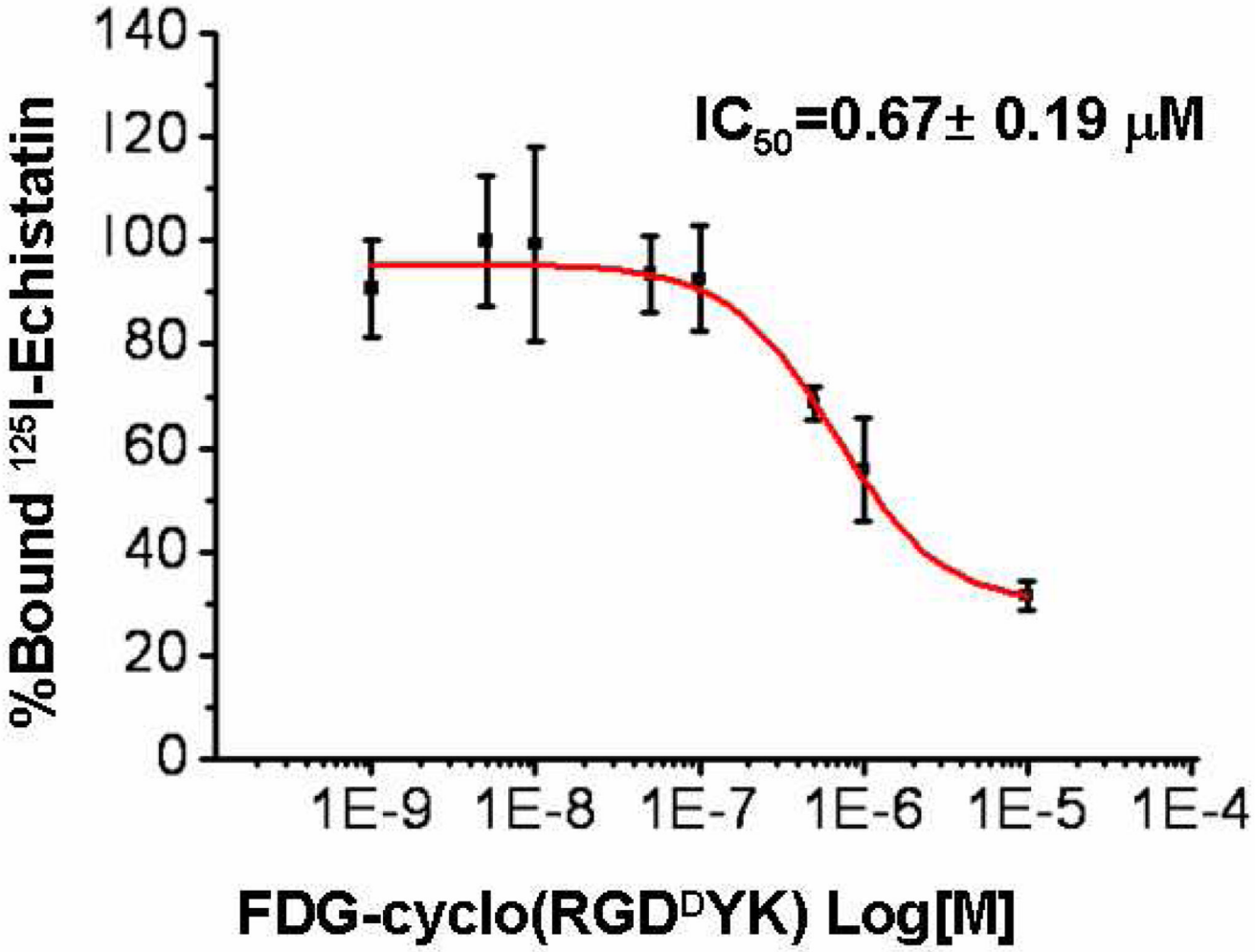

Figure 2.
Inhibition of ^{125}I-Echistatin (integrin $\alpha_v\beta_3$-specific) binding to $\alpha_v\beta_3$ intgrin on U87MG cells by FDG-cyclo(RGD^{D}YK).

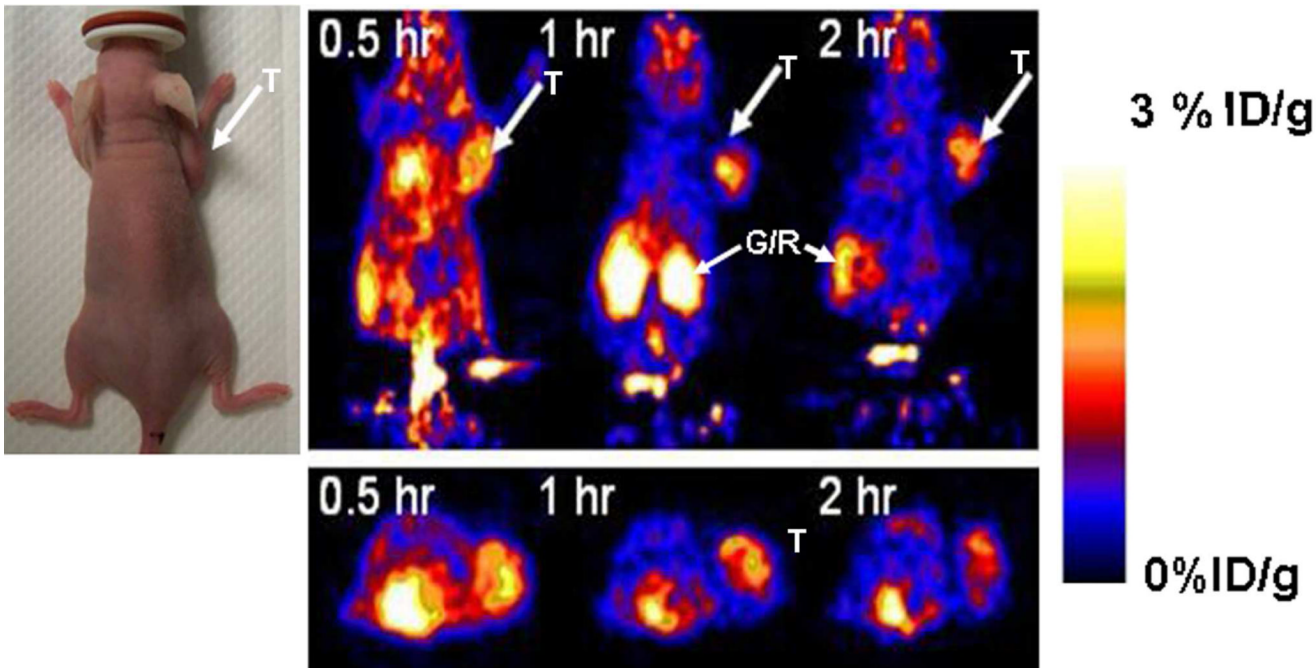

Figure 3.
Decay–corrected microPET images (coronal top and trnsaxial bottom) of a nude mouse (photograph shown on left) bearing U87MG xenograft at 0.5, 1 and 2 h after tail injection of 100 μCi of [^{18}F]FDG-RGD. T is for tumor, G/R is gastrointestinal/renal activities and color bar represents % ID/g.

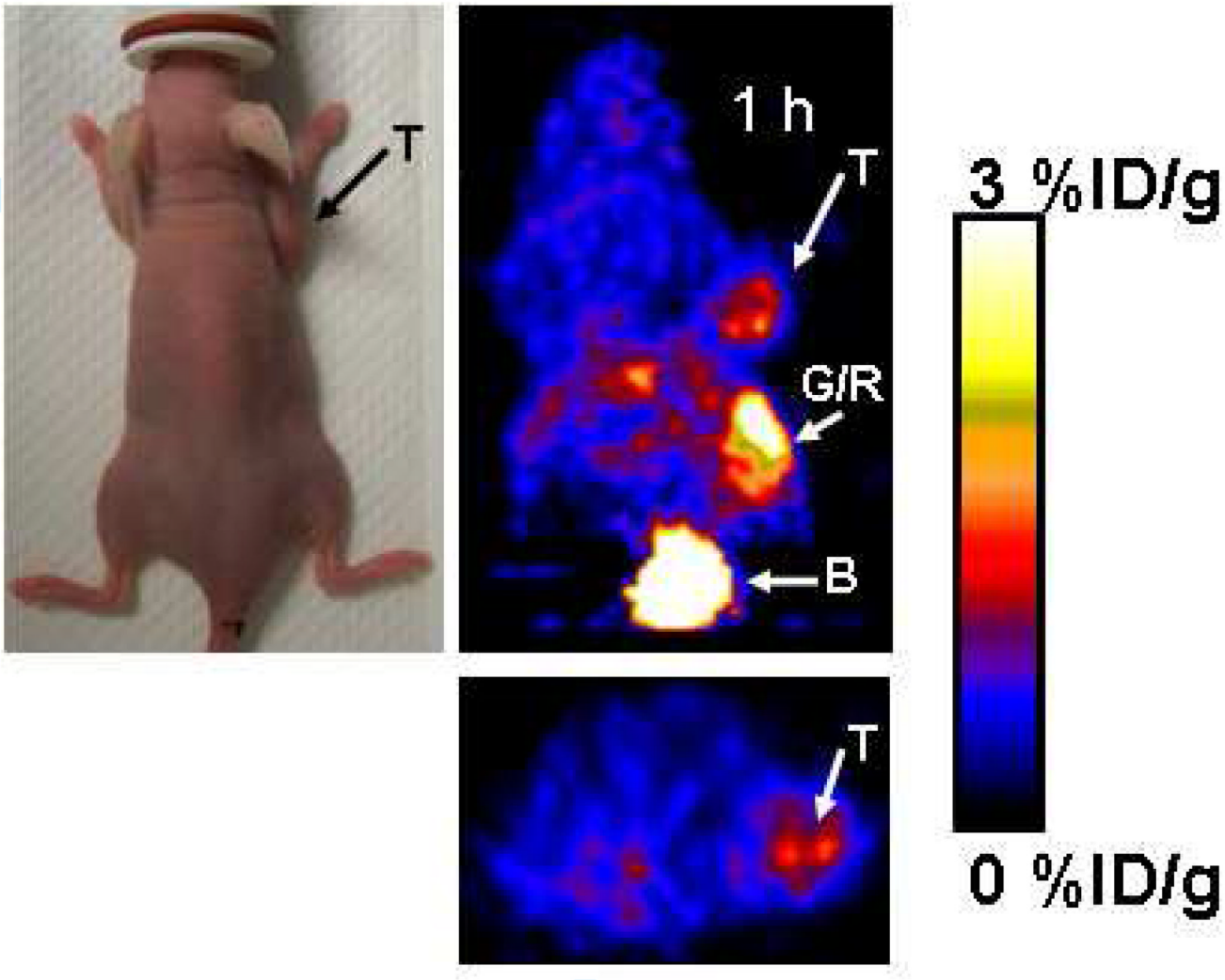

Figure 4.
Decay–corrected microPET images (coronal top and trnsaxial bottom) of a nude mouse bearing a U87MG xenograft at 1 h after tail injection of 72 μCi of [^{18}F]FDG-cyclo(RGD^{D}YK). T, tumor; B, bladder; G/R, gastrointestinal/renal activities and color bar represents % ID/g.

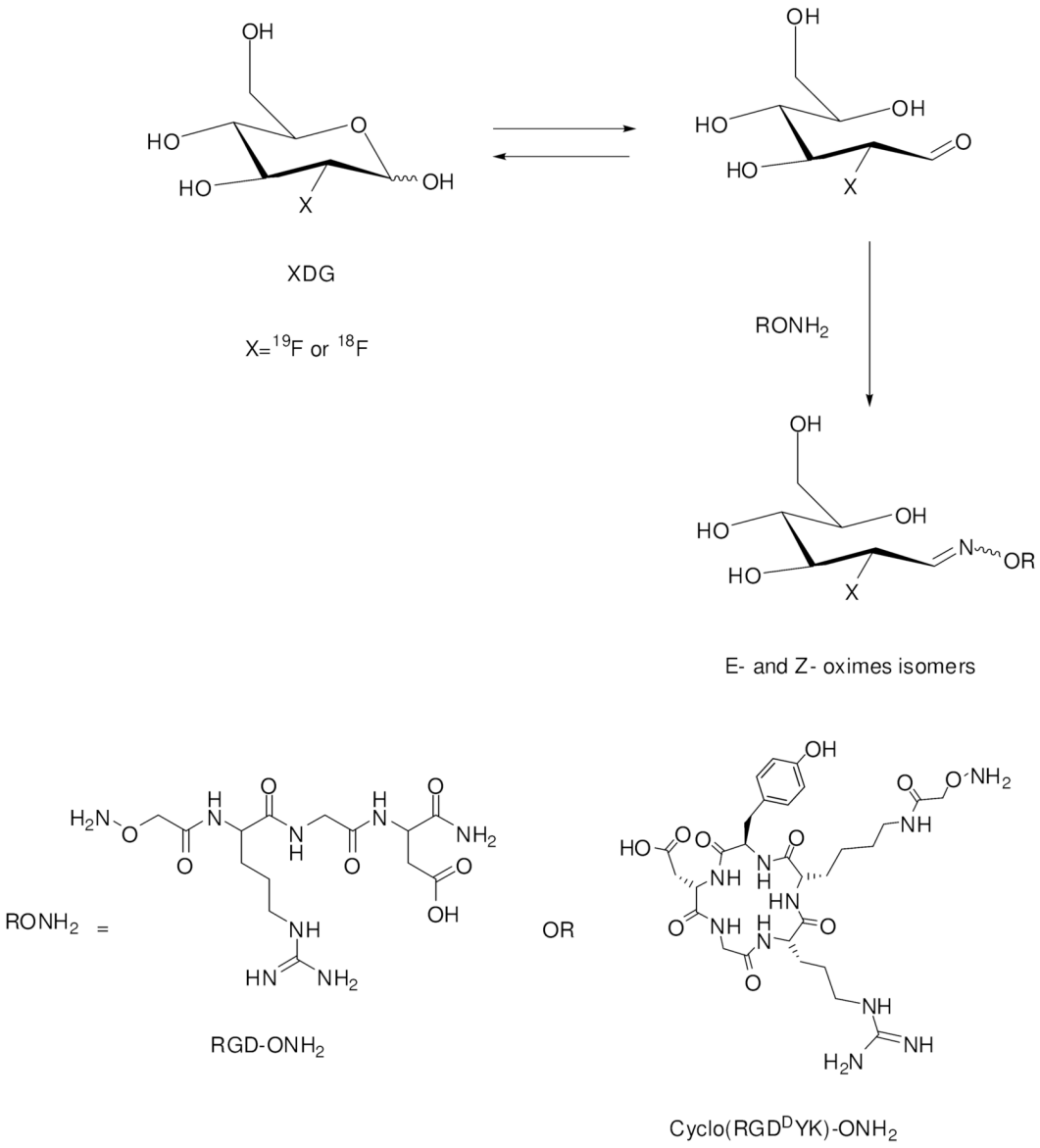

Scheme 1.

Schematic synthesis of FDG-RGD and FDG-cyclo(RGD^{D}YK) (X=^{19}F) from FDG or [^{18}F] FDG- RGD and [^{18}F]FDG-cyclo(RGD^{D}YK) (X=^{18}F) from [^{18}F]FGD.

Table 1

Biodistribution of [^{18}F]FDG- RGD in mice bearing U87MG xenografts. Data are expressed as of percentage of injected radioactivity per gram of organ or tissue (% ID/g) after intravenous injection of [^{18}F]FDG- RGD (10–30 μCi) at different time post injection (N=3 for each group).

Organ (%ID/g)	**0.5 h**	**2 h**
U87MG	0.94 ± 0.25	0.27 ± 0.06
Blood	0.43 ± 0.05	0.02 ± 0.00
Heart	3.56 ± 1.11	3.67 ± 0.26
Liver	0.44 ± 0.03	0.22 ± 0.04
Lungs	0.78 ± 0.05	0.47 ± 0.37
Muscle	0.27 ± 0.07	0.09 ± 0.03
Kidney	1.95 ± 0.17	0.55 ± 0.51
Spleen	0.49 ± 0.10	0.64 ± 0.68
Brain	0.58 ± 0.04	0.16 ± 0.02
Intestine	0.32 ± 0.03	0.19 ± 0.09
Stomach	0.61 ± 0.50	0.30 ± 0.32
Bone	0.29 ± 0.03	0.23 ± 0.20
Ratios		
T/Blood	2.19 ± 0.55	13.27 ± 1.05
T/Muscle	3.71 ± 1.49	3.50 ± 1.90
T/Liver	2.17 ± 0.76	1.25 ± 0.08
T/Kidney	0.49 ± 0.14	0.74 ± 0.43

Table 2

Biodistribution of [^{18}F]FDG-cyclo(RGD^{D}YK) in mice bearing U87MG xenografts. Data are expressed as of percentage of injected radioactivity per gram of organ or tissue (% ID/g) after intravenous injection of [^{18}F]FDG- RGD (10–30 μCi) at different time post injection (N=3 for each group).

Organ (%ID/g)	0.5 hr	1hr	2 hr
Kidney	4.75 ±5.60	3.75 ± 1.42	16.1 ± 13.0
Liver	1.32 ± 1.3		0.43 ± 0.40
Brain	0.80 ± 1.09		0.13 ± 0.07
Heart	1.11 ± 0.22		2.57 ± 2.53
Lung	0.54 ± 45		0.60 ± 0.66
Muscle	0.30 ± 0.10		0.13 ± 0.06
Stomach	0.17 ± 0.03		0.46 ± 0.52
Intestine	0.50 ± 0.02		0.28 ± 0.19
Bone	0.71 ± 0.65		0.13 ± 0.21
Blood	2.04 ± 2.28	0.84 ± 0.19	0.54 ± 0.31
U87MG	0.63 ± 0.13	0.95 ± 0.40	1.53 ± 1.59
Spleen	0.19 ± 0.16		0.17 ± 0.20
Ratios			
T/Blood	0.32 ± 0.17	1.19 ± 0.63	2.75 ± 1.62
T/Muscle	3.72 ± 2.16		12.9 ± 9.41
T/Liver	0.49 ± 0.30		6.02 ± 6.08
T/Kidney	0.15 ± 0.08	0.28 ± 0.17	0.17 ± 0.08